Coevolution of synchronous activity and connectivity in coupled chaotic oscillators

Li Chen,[1] Can Qiu,[1] Hongbin Huang,[1,*] Guanxiao Qi,[2] and Haijun Wang[3]
[1]*Department of Physics, Southeast University, Nanjing 210096, China*
[2]*Research Center Jülich, Institute for Neuronscience and Medicine INM-2, D-52425 Jülich, Germany*
[3]*Department of Physics, Nanjing Xiaozhuang College, Nanjing 210017, China*
(Received 5 July 2010; revised manuscript received 2 October 2010; published 18 November 2010)

We investigate the coevolution dynamics of node activities and coupling strengths in coupled chaotic oscillators via a simple threshold adaptive scheme. The coupling strength is synchronous activity regulated, which in turn is able to boost the synchronization remarkably. In the case of weak coupling, the globally coupled oscillators present a highly clustered functional connectivity with a power-law distribution in the tail with $\gamma \simeq 3.1$, while for strong coupling, they self-organize into a network with a heterogeneously rich connectivity at the onset of synchronization but exhibit rather sparse structure to maintain the synchronization in noisy environment. The relevance of the results is briefly discussed.

DOI: 10.1103/PhysRevE.82.056115 PACS number(s): 89.75.Fb, 05.45.Xt

Complex networks pervade all sciences and have proven to be productive to understand the sophisticated collaborative dynamics across many disciplines [1]. One interesting phenomenon observed in real-world networks is that the evolution of the connectivity is closely related to the activities of their nodes and vice versa. For example, recent neurophysiological evidences reveal that the development of neuron connections in central nervous systems is modulated by the neural activity [2], and the activity relies on the neural circuits conversely. The coevolution of the network connectivity and node activity has also been found in social [3,4], ecological [5], and epidemic networks [6,7], where agents or species learn from the state of networks and adapt their behaviors accordingly for interest or survival, which in turn reshape the structure of networks. Such *coevolutionary* or *adaptive* networks can provide us a more complete understanding of the collective dynamics, and from this perspective many interesting phenomena have been revealed, such as self-organized criticality and phase transitions (for a review, see [8]).

So far, the study of coevolutionary dynamics of coupled chaotic oscillators is just at its beginning, with special interests in maintaining or enhancing synchronization as well as the spontaneous structure formation. In [9] a potential-based adaptation strategy was proposed to maintain synchronization in the presence of exogenous unpredictable influences, and in [10] an adaptive feedback scheme was used to enhance synchronization by reducing the network heterogeneity. These two adaptive methods are though a set of auxiliary differential equations to control the network coupling dynamics. On the other hand, a globally coupled chaotic map with Hebbian-like dynamic connections can self-organize into an ever changing network structure of two distinct classes of nodes but only in asynchronous region [11]. Here, an issue of importance that arises is to elucidate the role of the interplay between the synchronous activity and the connectivity in such networks, which is also very relevant to brain dysfunctions. For instance, it is well acknowledged that the emergence of several psychiatric disorders is accompanied by pathological network topology and abnormal synchrony in brain, while the underlining mechanism at the network level is largely unknown (e.g., schizophrenia, Alzheimer disease, and epilepsy) [12]. Here considering a simple model as a first step we attempt to make a progress toward this goal.

In this paper, we present a threshold adaptive coupling scheme according to local synchronous activities, and focus on the impacts of the adaptation on network synchronization and self-organization. We mainly show that the adaptation facilitates the network synchronization remarkably, and the network self-organizes into distinct connectivities in different cases of synchronous activities.

Let us consider a network of N coupled identical chaotic oscillators

$$\dot{\mathbf{x}}_i = \mathbf{F}(\mathbf{x}_i) + \sum_{j=1}^{N} a_{ij}\varepsilon_{ij}(t)[\mathbf{H}(\mathbf{x}_j) - \mathbf{H}(\mathbf{x}_i)], \tag{1}$$

where $\mathbf{x} \in \mathbb{R}^m$ is the m-dimensional vector describing the state of nodes, $\mathbf{F}(\mathbf{x}): \mathbb{R}^m \to \mathbb{R}^m$ governs the local dynamics of the oscillators, $\mathbf{H}(\mathbf{x}): \mathbb{R}^m \to \mathbb{R}^m$ is a vectorial output function, and $A=(a_{ij})$ is the binary adjacency matrix determined by the underlining physical or structural connections.

Here, $\varepsilon_{ij}(t)$ is the time-varying coupling strength depending on synchronous activities of the two linked oscillators. Considering there is a limited resource in the real world, it is reasonable to assume that the coupling is completely activated only when some thresholds are exceeded (e.g., spike discharge for neurons). The following are the connection strengths by incorporating this dynamic factor:

$$\varepsilon_{ij} = \varepsilon_0 S\left(\frac{|\Delta w_{ij}|}{|\Delta w'_{ij}|} - l\right), \tag{2}$$

where ε_0 is the maximal strength of coupling that the interacting channel can provide. The coupling dynamic is modeled by a sigmoid function $S(x)=1/(1+e^{-\alpha x})$, with α controlling the smoothness between 0 and 1 [a limiting version of $S(x)$ is the Heaviside function as $\alpha \to +\infty$] [13]. Hereafter, we choose $\alpha=10$. Δw_{ij} represents the state difference of the di-

*hongbinh@seu.edu.cn

 ©2010 The American Physical Society

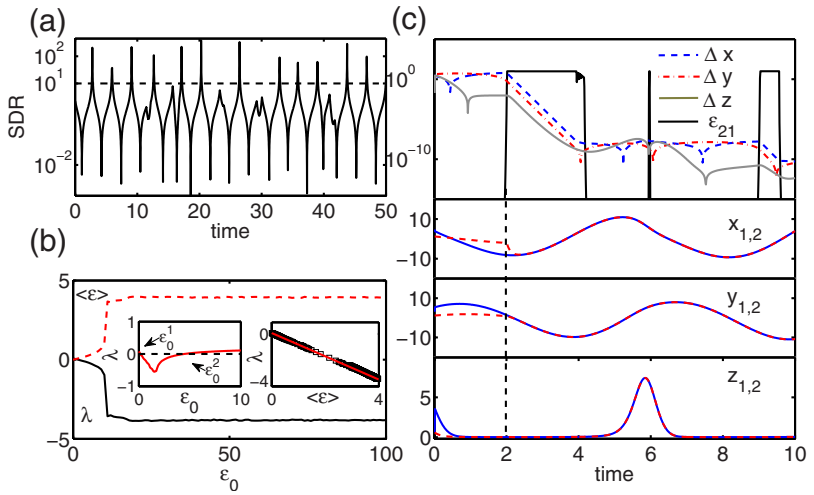

FIG. 1. (Color online) (a) The plot of $|\Delta w_{12}|/|\Delta w'_{12}|$ for two uncoupled Rössler oscillators. (b) LLE λ (black solid) and average coupling strength $\langle\varepsilon\rangle$ (red dashed) as a function of ε_0 ($\varepsilon_0^c \simeq 1.6$). Left inset: LLE with the constant coupling strength as a function of ε_0. Right inset: LLE λ vs average coupling strength $\langle\varepsilon\rangle$ (red fitted line corresponds to constant vector coupling case). Time step $\Delta t=0.001$. (c) Coevolution in transition to synchronization in two unidirectional coupled Rössler oscillators with $\varepsilon_0=10$. Upper panel: time evolution of coupling strength and variable differences; lower panels: time series.

rectly coupled dynamical variable between nodes i and j, and $\Delta w'_{ij}$ are those corresponding to the rest variables. Here we call $|\Delta w_{ij}|/|\Delta w'_{ij}|$ the state difference ratio (SDR). The parameter l is the threshold that controls the activation of the coupling and a larger l means less chance of activation. In the following we will show that the adaptive coupling described by the simple Eq. (2) can boost network synchronization dramatically, no other auxiliary equations are needed.

For the sake of simplicity, we begin with the case of two unidirectionally coupled chaotic oscillators (i.e., $a_{12}=0$ and $a_{21}=1$ with $N=2$). In this case, the stability of synchronous states can be assessed by studying the variational equations of Eq. (1) with respect to the synchronous manifold $\dot{\mathbf{x}}_1=\mathbf{F}(\mathbf{x}_1)$

$$\Delta\dot{\mathbf{x}} = [\mathbf{DF}(\mathbf{x}_1) - \varepsilon_{21}\mathbf{DH}(\mathbf{x}_1)]\Delta\mathbf{x}, \tag{3}$$

where $\Delta\mathbf{x}=\mathbf{x}_1-\mathbf{x}_2$ and $\mathbf{D}$ is the Jacobian operator. The stability problem is then reduced to calculate the largest Lyapunov exponent (LLE) $\lambda=\lim_{t\to\infty}\frac{1}{t}\ln|\frac{\Delta\mathbf{x}(t)}{\Delta\mathbf{x}(0)}|$ of Eq. (3); the synchronous state is stable if $\lambda<0$, and unstable if $\lambda>0$. Furthermore, according to the definition of LLE, a more negative λ will lead to a higher converging speed of synchronization.

To be specific, we adopt the chaotic Rössler oscillator throughout the study when not stated otherwise: $\mathbf{x}=(x,y,z)$ and $\mathbf{F}(\mathbf{x})=[-y-z,x+0.2y,0.2+z(x-7)]$, with $\mathbf{H}(\mathbf{x})=(x,0,0)$, in this case $w=x$ and $w'=(y,z)$. The threshold l is chosen such that SDR can reach the threshold in typical time scale of the oscillator. A proper choice can be made by referring to the plot of SDR for two completely uncoupled oscillators and l is chose in the range of SDR, in the present case we set $l=10$ [see Fig. 1(a)]. In Eq. (2) $|.|$ denotes the norm defined as $|\Delta w'_{ij}|=\max(|\Delta y_{ij}|,|\Delta z_{ij}|)$, though the results described below do not change qualitatively for other choices of norm.

It is known that the synchronization for the case of x-coupled Rössler oscillators with traditional constant coupling [without $S(x)$ in Eq. (2)] is only stable for intermediate coupling strength due to the short or long wavelength bifurcation [14] and the stable synchronous region is thus bounded $\varepsilon_0^1<\varepsilon<\varepsilon_0^2$ [left inset in Fig. 1(b)]. Surprisingly, the synchronization ability is strikingly boosted when the coupling strength is modulated by the $S(x)$.

Figure 1(b) reports the performance by varying ε_0. The first crucial observation in Fig. 1(b) is that the second cross point ε_0^2 disappears and the stable region becomes unbounded. Also, the absolute value of LLE shown in Fig. 1(b) is about one order larger than that of constant coupling case, which means a much higher converging speed for proper ε_0 (note the logarithmic definition of LLE). Another quantity we concern is the effective coupling cost consumed in reality. A convenient way is to define the average coupling strength $\langle\varepsilon\rangle=\lim_{\tau\to\infty}\frac{1}{\tau}\int_{t_0}^{t_0+\tau}\varepsilon_{21}dt$. The result in Fig. 1(b) shows that actually very low coupling cost is needed although the maximal coupling strength ε_0 that the channel provides could be extremely strong. More interestingly, there is a linear relationship between λ and $\langle\varepsilon\rangle$, which can be well fitted by the constant vector coupling case [right inset in Fig. 1(b)]. This behavior can be explained easily. When in inactivation for duration denoted by t_i, the two oscillators are uncoupled and the variable difference $\Delta\mathbf{x}$ evolves as $e^{\lambda_0 t_i}$, where λ_0 is the LLE for the sole oscillator. And when the coupling is fully activated for duration t_a, since now $\Delta x>10\max(\Delta y,\Delta z)$, the difference $\Delta\mathbf{x}\simeq\Delta x$, and $\Delta\dot{x}\simeq-\varepsilon_0\Delta x$ if ε_0 is not too small. These suggest that $\Delta\mathbf{x}$ in this process evolves as $e^{-\varepsilon_0 t_a}$. Taken together, the average evolution then can be expressed by $\Delta\mathbf{x}(t)\sim\exp[(\lambda_0\frac{t_i}{t_i+t_a}-\varepsilon_0\frac{t_a}{t_i+t_a})t]$, and by taking into account $t_i\gg t_a$ and $\varepsilon_0\frac{t_a}{t_i+t_a}=\langle\varepsilon\rangle$ we thus have

$$\lambda \simeq \lambda_0 - \langle\varepsilon\rangle, \tag{4}$$

which indicates that the adaptive coupling is as effective as the constant vector coupling case $[\mathbf{H}(\mathbf{x})=\mathbf{x}=(x,y,z)]$.

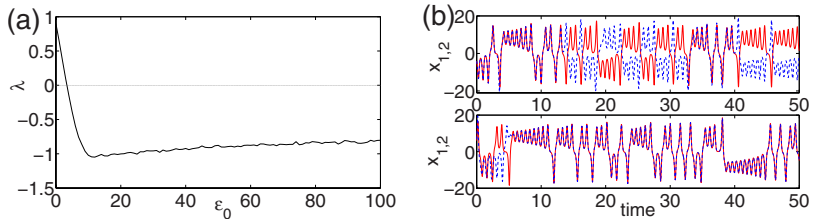

FIG. 2. (Color online) (a) LLE λ as a function of ε_0 for z-coupled Lorenz oscillators. (b) Time series with $\varepsilon_0=10$ in noisy background $\sim 10^{-5}$. Upper panel: constant coupling; lower panels: dynamic coupling with Eq. (2). Here the threshold $l=2$.

Figure 1(c) illustrates the coevolution of the coupling strength and node activities in typical transition to synchronization. Most of the time, the connection strength is very small and the interacting channel is closed. Once the interacting channel is triggered (see, e.g., an onset of the coupling activation indicated by the dashed line at $t=2$), the increased coupling strength can effectively reduce their state differences.

In fact, the mechanism discussed above is general and not restricted to the specific choice of chaotic oscillators. In numerical simulations, we found that it can be applied to a variety of typical chaotic oscillators, such as Lorenz oscillators, Chen systems, Chua's circuit systems, etc. As another example, z-coupled Lorenz equations $\mathbf{F}(\mathbf{x})=[10(y-x),28x-y-xz,xy-8/3z]$, with $\mathbf{H}(\mathbf{x})=(0,0,z)$, show that the synchronization and anti-synchronization coexist in noisy environments due to the symmetry $(x,y,z)\rightarrow(-x,-y,z)$ for constant coupling and the negative region of the LLE is bounded [15]. Nevertheless, the LLE with the dynamic coupling [Eq. (2)] become wide stable region, and more importantly the antisynchronization is now excluded, see Fig. 2.

Now we turn to consider a globally coupled network with

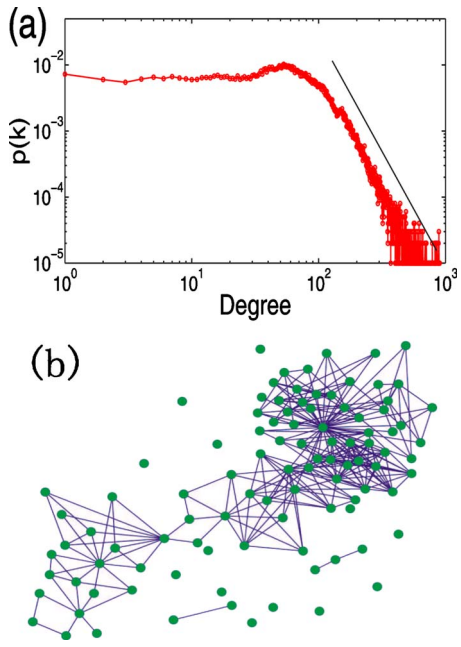

FIG. 3. (Color online) (a) Connectivity distribution for weak synchronization (average over 100 realizations). (b) A snapshot of the evolving network with $N=100$ and $\varepsilon=0.1$ [17].

$N=1000$, in which any two nodes are assumed to have a structural channel (i.e., $a_{ij}=1$, $\forall i\neq j$). Because the network is inherently dynamic in connection strengths, here we focus on the pattern of real-time connectivity, i.e., functional connectivity. To do this, we define that two nodes are functionally connected if their coupling strength exceeds a predetermined value ε_c. In the simulation, we set $\varepsilon_c=\varepsilon_0/100$ [16].

We begin with weak synchronization with $\varepsilon_0=0.01$. In this case, huge networks can be synchronous even for very small ε_0 (in simulation $\varepsilon_0\gtrsim\varepsilon_0^c/N$). However, due to the low synchronous speed, very long converging time is required, and thus the global synchronization is unlikely to happen in reasonably short time. In this sense, we say weak synchronization. In numerical simulation, we find that the resulting functional network displays a continuous, ever changing evolution, in which a node is a hub at one time could become a peripheral, even isolated one at another time. The degree distribution $p(k)$ shows a skewed distribution in the tail approaching $p(k)\sim k^{-\gamma}$, with $\gamma\simeq 3.1$ [Fig. 3(a)]. This power law implies that there is always a small fraction of nodes emerging as "leaders" in the evolution and the functional networks have the property of scale-free [18]. Further studies show that the clustering coefficient of functional networks is much lager than its random equivalent network (Table I), obtained by randomly rewiring the links of the original networks while keeping their total degree. A typical snapshot of the connectivity is given in Fig. 3(b), which is composed of a giant component, some small clusters, and some isolated nodes.

Different from the weak synchronous case, the strong synchronization induced by large coupling can rapidly reduce the state difference, and the global synchronization is thus expected in short time. Figure 4 reports coevolutionary behaviors with $\varepsilon_0=1$ by considering the background noise as well as local external stimulus. As shown in Fig. 4(a), the synchronous activities can be classified into three phases: onset, maintenance, and stimulus. In the onset phase (phase I), the synchronous error $e(t)$ decreases sharply to the limiting level (determined by the noise level as well as the net-

TABLE I. Statistical properties of the resulting functional networks for weak and strong synchronization (phases I [19] and II).

Sync activities	Weak sync	Strong sync I	Strong sync II
$\langle k\rangle$	94.1	137.0	3.7
C	0.6	0.52	0.19
C_{rand}	0.094	0.137	0.0033

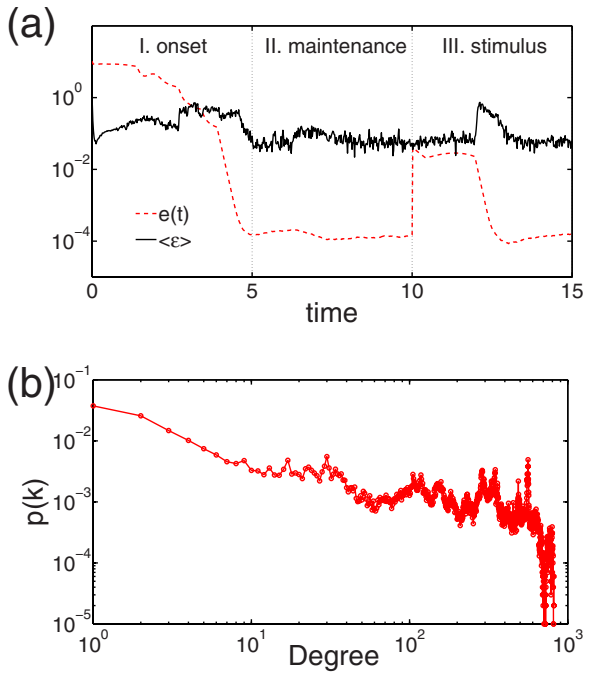

FIG. 4. (Color online) (a) Time evolution of synchronous error $e(t)$ and the average coupling strength $\langle\varepsilon\rangle$ for strong synchronization in the presence of background noise $\sim 10^{-5}$. An external stimulus $\sim 10^{-2}$ is added to one of the nodes at $t=10s$. Here, $e(t)=\frac{1}{N}\Sigma_{i=1}^{N}(|x_i-\bar{x}|+|y_i-\bar{y}|+|z_i-\bar{z}|)$, with $\bar{u}=\frac{1}{N}\Sigma_{i=1}^{N}u_i, u=x,y,z$ and $\langle\varepsilon\rangle=\frac{1}{N(N-1)}\Sigma_{i,j=1}^{N}\varepsilon_{ij}$. (b) Connectivity distribution in the onset phase (average over 100 realizations).

work size N), accompanied by the high level of channel activations, which is reflected by the increase in average coupling strength and the rich network connectivity (Table I). The degree distribution shows that the functional network is heterogeneous but not scale-free, and considerable parts of nodes have large degree [Fig. 4(b)]. Once $e(t)$ reaches the limiting level, only very low coupling cost is needed to maintain the synchronous state (phase II), and the resulting network is rather sparse (Table I). However, such coevolutionary network is robust and very economical to background noise, but costly to external stimulus (phase III), even a local stimulus can trigger a burst of intensive activation of coupling. Interestingly, the coupling channels of the network are not activated immediately when they receive the stimulus, but keep its low channel activity for a delay until the right time. Statistical properties in Table I show that the average degree $\langle k\rangle$ decreases dramatically in phase II compared to that of phase I, and the clustering coefficients C in strong synchronization cases is smaller than that of weak case, but much larger than their random equivalent networks C_{rand}.

In summary, we have investigated coevolutionary dynamics by incorporating a threshold coupling and found that the adaptive strategy can give rise to unbounded stable region for chaotic synchronization, high converging speed, and low effective coupling cost. Within the model, the globally coupled oscillators produce very different functional networks in different cases of network synchronous activities. For the weak coupling, the connectivity shows a power-law distribution in the tail with high clustering, while for strong-coupling case, the network self-organizes into heterogeneously rich connectivity at the onset of synchronization but exhibits rather sparse structure to maintain synchronization in noisy environment. However, the adaptive network synchronization or connectivity is economical to background noise, but costly to external stimulus.

Currently, there is yet little known about the interdependency between the network connectivity and the node activity [1]. We believe that our model provides a promising framework for understanding the realistic networked systems, e.g., some brain diseases [20,21], in which different (health or abnormal) brain states may correspond to different coupling circumstances. In any case, a more in-depth understanding of the mechanisms of brain diseases will be possible only through the combination of theoretical and experimental studies and remains a big challenge in future.

[1] S. Boccaletti *et al.*, Phys. Rep. **424**, 175 (2006).
[2] J. Y. Hua and S. J. Smith, Nat. Rev. Neurosci. **7**, 327 (2004).
[3] B. Skyrms and R. Pemantle, Proc. Natl. Acad. Sci. U.S.A. **97**, 9340 (2000).
[4] A. W. Lo, J. Portfol. Manage. **30**, 15 (2004).
[5] U. Dieckmann and M. Doebeli, Nature (London) **400**, 354 (1999).
[6] T. Gross, Carlos J. Dommar D' Lima, and B. Blasius, Phys. Rev. Lett. **96**, 208701 (2006).
[7] S. Funk, E. Gilad, C. Watkins, and V. A. A. Jansen, Proc. Natl. Acad. Sci. U.S.A. **106**, 6872 (2009).
[8] T. Gross and B. Blasius, J. R. Soc., Interface **5**, 259 (2008).
[9] F. Sorrentino and E. Ott, Phys. Rev. Lett. **100**, 114101 (2008).
[10] C. S. Zhou and J. Kurths, Phys. Rev. Lett. **96**, 164102 (2006).
[11] J. Ito and K. Kaneko, Phys. Rev. Lett. **88**, 028701 (2001).
[12] F. Varela *et al.*, Nat. Rev. Neurosci. **2**, 229 (2001); O. Sporns *et al.*, Trends Cogn. Sci. **8**, 418 (2004); P. J. Uhlhaas and W. Singer, Neuron **52**, 155 (2006); E. Bullmore and O. Sporns, Nat. Rev. Neurosci. **10**, 186 (2009).
[13] Similar coupling function can be found in modeling excitatory chemical synapses, known as the fast threshold modulation [see D. Somers and N. Kopell, Biol. Cybern. **68**, 393 (1993)]. Notably, the essential difference in our modeling is that only the coupling strengths are modulated by the function rather than the whole coupling term.
[14] J. F. Heagy, L. M. Pecora, and T. L. Carroll, Phys. Rev. Lett. **74**, 4185 (1995).
[15] L. Huang, Q. Chen, Y. C. Lai, and L. M. Pecora, Phys. Rev. E **80**, 036204 (2009).
[16] The study has also been conducted for other ε_c, and qualitatively similar behavior is observed. This occurs because most

of the time-varying coupling strengths are either close to ε_0 or extremely small. One exception is at the onset stage of strong synchronziation [phase I in Fig. 4(a)], in which if $\varepsilon_c < \varepsilon_0/10$, the network connectivity observably reduces. However, the effect of ε_c is gone when α becomes larger.

[17] There is a scaling relation between the network size and the coupling strength $\varepsilon_1 N_1 = \varepsilon_2 N_2$, for which the two networks have qualitatively the same behaviors.

[18] A.-L. Barabási and R. Albert, Science **286**, 509 (1999).

[19] In phase I, the average data collected in 1–4 s excludes the beginning waiting stage and some advanced maintaining state. In fact, in this phase there is an intensive burst of coupling and the maximal average degree can reach nearly 500, half of the network size. Details will be published elsewhere.

[20] M. Chavez, M. Valencia, V. Navarro, V. Latora, and J. Martinerie, Phys. Rev. Lett. **104**, 118701 (2010).

[21] V. M. Eguiluz, D. R. Chialvo, G. A. Cecchi, M. Baliki, and A. V. Apkarian, Phys. Rev. Lett. **94**, 018102 (2005).